Time-resolved measurements of modulated breathing oscillations in Cylindrical Hall Thruster

IEPC-2017-267

Presented at the 35th International Electric Propulsion Conference
Georgia Institute of Technology • Atlanta, Georgia • USA
October 8 – 12, 2017

I. Romadanov[1]
University of Saskatchewan, Saskatoon, SK, S7N 5E2, Canada

Y. Raitses[2], A. Diallo[3], I. Kaganovich[4]
Princeton Plasma Physics Laboratory, Princeton, New Jersey, 08540, USA

K. Hara[5]
Texas A&M University, College Station, Texas, 77843, USA

and

A. Smolyakov[6]
University of Saskatchewan, Saskatoon, SK, S7N 5E2, Canada

Abstract: Time-resolved laser-induced fluorescence technique was implemented in cylindrical Hall thruster to study discharge current oscillations. These oscillations were the result of the coupling between natural breathing oscillations and the external sinusoidal driving of the anode potential. External driving frequency was around the intrinsic breathing mode frequency ~ 13 kHz. External driving forced natural oscillations to become coherent in time, and allowed to study the time evolution of xenon ion velocity distribution functions at different phases of the discharge current cycle. Different amplitudes of the anode potential driving were tested and it was shown that such driving can be used to control thruster behavior without changes in averaged plasma parameters. 1D hybrid simulations were performed and results were compared to experiments.

[1] PhD student, Department of Physics and Engineering Physics, ivr509@mail.usask.ca.
[2] Principal Research Physicist, Plasma Physics Laboratory, yraitses@pppl.gov.
[3] Staff Research Physicist, Plasma Physics Laboratory, ikaganovich@pppl.gov.
[4] Principal Research Physicist, Plasma Physics Laboratory, adiallo@pppl.gov.
[5] Assistant Professor, Department of Aerospace Engineering, khara@tamu.edu
[6] Professor, Department of Physics and Engineering Physics, andrei.smolyakov@usask.ca.

I. Introduction

Hall thrusters is a class of plasma propulsion device which has been used for different space missions[1]. Detailed description of their design and operation can be found, for example in Ref. 2, 3. Plasmas in Hall thrusters prone to various oscillations over a wide frequency range[4]. Oscillations at about tens of kilohertz have the most drastic effect on the thruster operation[4, 5]. There are two main types of modes in this frequency range: breathing and spoke. Breathing mode propagates in axial direction[6-8] with m = 0 (m is the azimuthal mode number), and spoke mode[9, 10] propagate in azimuthal direction with m = 1 or above. In this study, we focused on breathing oscillations, because they have bigger impact on the discharge parameters, and can lead to an interruption of the discharge. Such oscillations manifest themselves in a change of the discharge current, and their appearance is associated with plasma instability of the ionization region into the thruster channel[11].
Despite many theoretical and experimental works related to these modes, a full understanding of the physical mechanisms that lead to their occurrence is still missing. Especially, effects of these modes on the ion dynamics. Therefore, evolution of the ion velocity distribution function (IVDF) can help to improve a theoretical model and serve for verification of numerical simulations.

A method of time-resolver laser-induced fluorescence (TR-LIF) technique, which allows to measure IVDFs at different phases of the discharge is presented in this paper. This method consists of two parts: optical setup, and electrical circuit, which provides driving and ensure coherence between laser modulation and anode potential driving. Natural oscillations in plasma are non-stationary, and not coherent in time, meaning that frequency and phase vary around some characteristic values. In order to obtain time-coherent oscillations in plasma, it was externally driven with sinusoidal wave on frequency around naturally occurred breathing oscillations; therefore, observed fluctuations were the result of coupling of these modes. The coupling to the breathing mode is essential to the used diagnostic scheme.

Laser-induced fluorescence (LIF) is an optical diagnostic technique that allows to obtain the velocity distribution functions (VDF) of atoms or ions along the laser beam direction by measuring the Doppler shift. A continuous wave (CW) laser was used to probe a xenon ion population of $5d^2F_{7/2}$ to $6\mathrm{p}D^0{}_{5/2}$ transition by 834.953 nm wavelength. Laser light was modulated at frequency half of the anode potential driving frequency; absolute phase shift between driving and laser signals was controlled to obtain LIF signal at particular time point of the discharge cycle. LIF signal was extracted from the response of the photomultiplier tube (PMD) by use of phase-detection technique. This approach differs from the photon counting technique, which was used in Ref. 12, 13, or heterodyne approach, which was discussed in Ref. 14.

II. Experimental setup

These experiments were performed at the Princeton Plasma Physics Laboratory, at small Hall Thruster Experiment facility. Cylindrical Hall thruster with 2.6 cm channel diameter and was used during experiments. Detailed description of the design and operation can be found in Ref. 15, 16. Propellant was xenon-gas with flow rate through anode at 3.5 sccm and cathode at 2.0 sccm. The thruster was into 1.0 m length and 0.8 m diameter vacuum chamber, with vacuum supplied by turbopump, and steady state background pressure at about 6.0×10^{-5} Torr. Thruster was operated at 220 V anode potential; typical values of discharge current were approximately 0.8 A. Current on main magnetic coil current was 2.5 A and on the front magnetic coil current was 0.5 A in “direct” configuration, description of the magnetic field configurations is given in Ref. 15.

A. Electrical setup

Without external driving, the above combination of parameters caused a natural breathing oscillation at frequency around 13 kHz. However, these oscillations are not very coherent in time: frequency and phases change from cycle to cycle. To control the behavior (frequency, phase, and amplitude) of natural oscillations anode potential was modulated. A schematic view of the electrical setup is represented in Fig. 1. Amplifier is installed between the anode power supply and the anode. Sine wave from function generator is feed into it; therefore, anode potential became a shifted sine wave, with base line at 220 V. This procedure is very similar to one that was used in Ref. 14, 17.

The discharge current was constantly monitored during the experiments. Ion density probe was installed at 12 mm from the exit plane, and this data was collected as well.

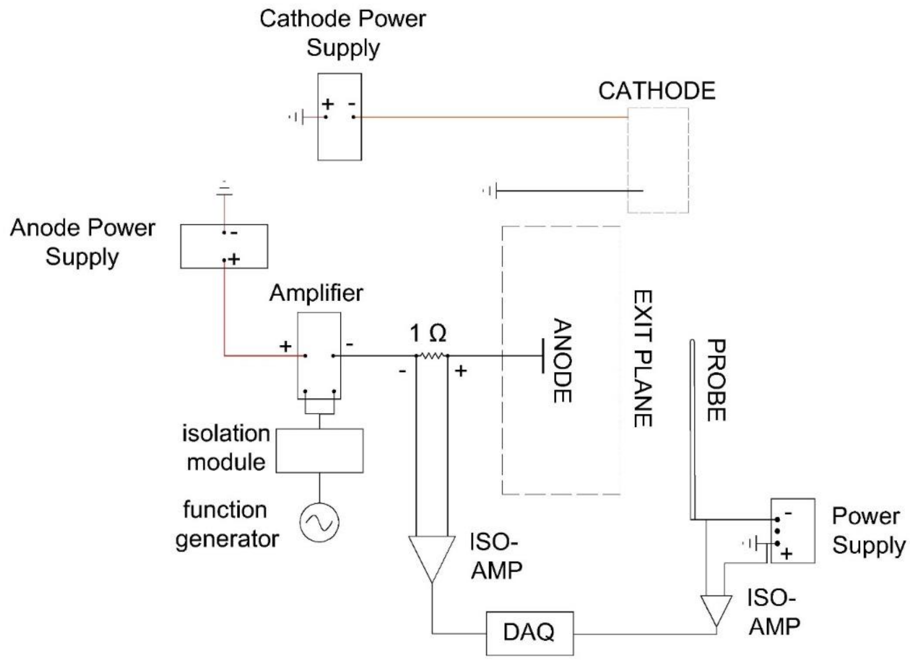

Figure 1. Electrical schematics of the anode driving system.

B. Optical setup

Optical setup for the LIF experiment is presented in Fig. 2. TLB-6917 Vortex™ II tunable diode laser produces pumping beam A at 834 nm wavelength with approximately 2 mm cross section diameter and 60 mW power. Laser light wavelength can be tuned in a range of hundredths of nm, which is enough to cover the velocities range of interest. Part of the laser beam is cut by the beam splitter (BS1) and sent into Bristol WM621 wavemeter/powermeter, by using an optical fiber. Laser wavelength is continuously measured during the experiment and deviations from the central frequency ensures that the velocity error is less than 16 m/s. Power of the beam is controlled during the experiment, but its drift is typically small over the time of measurement. After the beam splitter BS1 beam is sent into an acousto-optic modulator (AOM), where it is modulated. Modulation pulses come from the same function generator, which is used for anode potential driving. This allows to control the phase shift between them. However, frequency of the laser modulation is different. Modulation is necessary to distinguish between the fluorescence signal from laser and spontaneous plasma emission. AOM provides two beams: 0th and 1st order. Only 1st order beam is modulated, and 0th order beam is blocked by the iris. Second beam splitter (BS2) reflects a part of the beam into a fast photodiode (PD). Then the beam is sent through the collimating lenses (L1 & L2), and two mirrors (M1 & M2). After the mirror M2 beam entrances the chamber though the viewport, which is leveled below the thruster axis, so, beam is aligned inside the chamber, by turning prisms (M3 & M4), to coincide with the thruster axis. Lens L3 collects light from the point on the thruster axis and 12 mm away from the thruster exit plane. Laser beam at the collection point has power about 8 mW, which provides a good signal-to-noise ratio and no saturation of the transition. A combination of plano-convex lens L4 and iris collects light send this light into a collimation lens L5. Light is then passed into a photomultiplier tube (PMT) by two mirrors (M5 & M6). Desired wavelength is extracted from the collected light by 540 nm filter with 10 nm bandwidth.

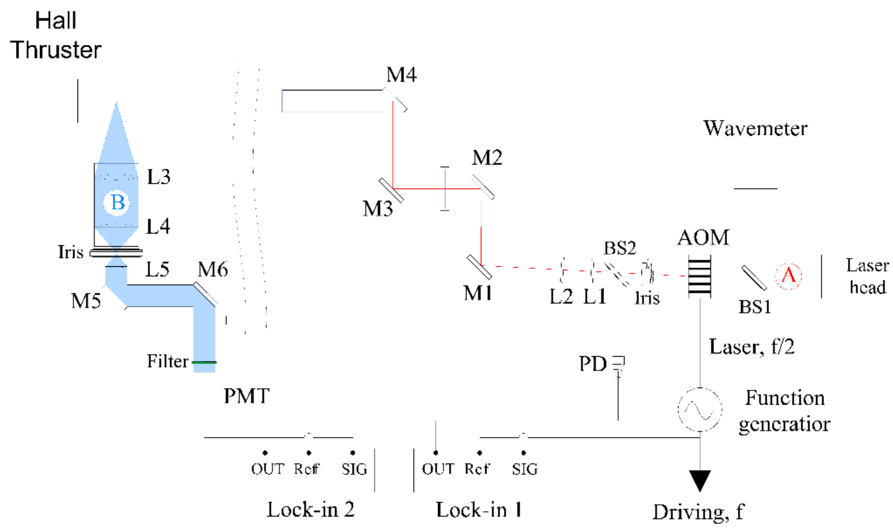

Figure 2. Optical setup for the LIF experiment. M1-6 – mirrors, BS1,2 – beam splitters, PD – photodiode, PMT – photomultiplier tube, AOM- acousto-optic modulator, L1,2 – collimating lenses, L3-5 – collection lenses, A – pump laser beam, B – LIF signal beam; f – anode potential driving frequency.

C. Diagnostic technique

First, frequency of the intrinsic breathing was determined by measuring of the discharge current and its spectrum. Example of the discharge current series and its Fourier transform is shown in Fig. 3a, b. There are peaks around 13-15 kHz. On the next step, the driving frequency was varied in this range and the discharge current and its spectrum were monitored. At constant amplitude of the driving voltage, the amplitude of the discharge current changes with the driving frequencies. Maximum of the amplitude was achieved at around 13 kHz, and this was defined as a coupling between external driving and natural mode. Driving of the potential even at a small amplitude results in highly coherent oscillation of the discharge current. Example of the discharge current trace and its spectrum at 16 V_{pp} amplitude driving is presented in Figure 3c, d. Hence, the optimal driving frequency is determined.

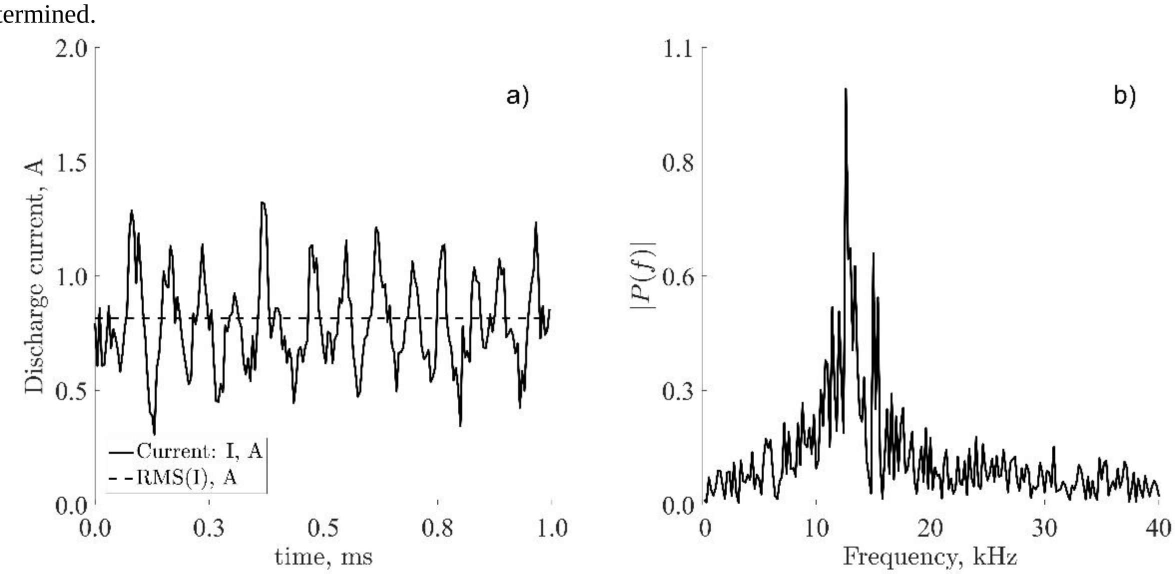

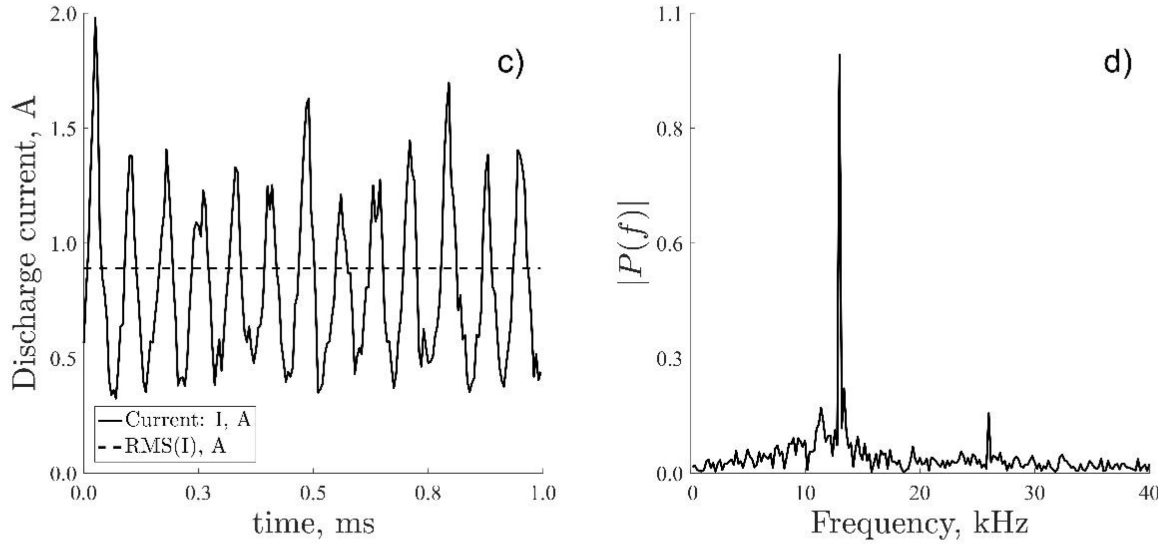

Figure 3. Discharge current traces without (a) and with (b) anode driving, and corresponding Fourier transforms (b, d).

There are several things to notice about the effects of the driving. First, it is clearly seen that discharge current oscillations become coherent in time; phase stays constant, and there is a prominent peak on frequency plot at the driving frequency (see Fig. 3d). Second, mean current value remain unchanged, even though amplitude became higher. It means, that external oscillations are coupled only with the breathing mode. Last two points ensures that the thruster time-average behavior is not affected by modulations. Moreover, this technique is based on an assumption that plasma properties are repeatable between discharge cycles.

To make measurements time-resolved, ions should be excited only at some particular time of the discharge cycle. Laser beam was modulated with short enough pulses to ensure that plasma parameters do not change. Length of the pulse was chosen to be long enough to provide a signal with acceptable signal-to-noise ratio. In general, length of the pulse is limited by the laser beam power. Discharge current oscillation and laser pulses with respect to each other for two cases, at maximum and minimum of the discharge, are shown in Fig. 4.

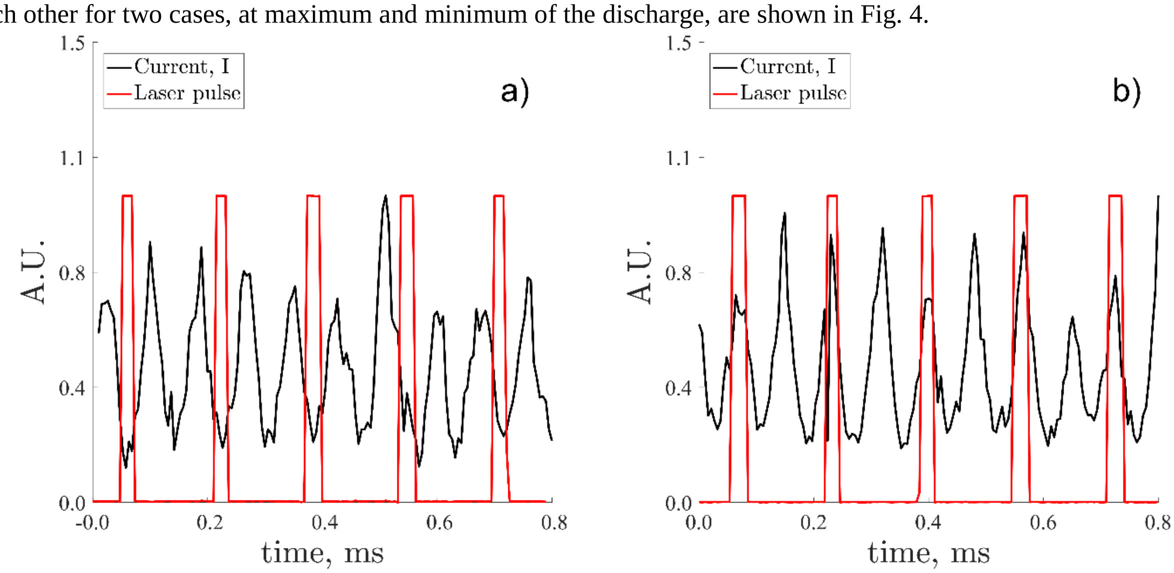

Figure 4. Discharge current oscillation and laser pulses with respect to each other for lowest (a) and highest (b) points of the discharge currents oscillations.

Because of the breathing modes, density of ion population oscillates in time; therefore, intensity of the emitted light changes in time, and PMT response becomes periodical. Laser beam excites metastable ions, which emit light, at AOM modulation frequency. Consequently, PMT signal contains two periodical signals in it: one from naturally emitted light and another one from the laser induced light. Signal from the photodiode PD goes into first lock-in amplifier to generate a reference signal. Signal from the PMT is sent into the second lock-in amplifier, which extracts the LIF signal from it, by using frequency and phase of the reference signal. So, to distinguish between these two signals, the laser beam was modulated at a frequency equal to a half of the thruster driving frequency. Location of the laser pulse along the discharge cycle was controlled by the phase shift between two signals.

III. Experimental results

Experiments were performed with different values of the driving amplitude potential, and LIF signal was measured at highest and lowest points of the discharge current cycle. This allowed to track the temporal evolution of IVDF at different phases of the discharge, and study the effect of the breathing mode amplitude. Figure 5 shows the time-resolved IVDF at 16 V_{pp} driving voltage amplitude at lowest and highest points of the discharge. IVDFs on lower amplitudes look very similar, and not shown here

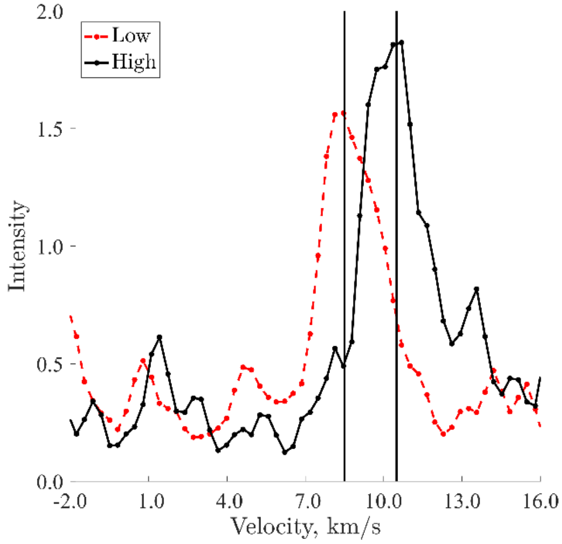

Figure 5. Velocity distribution functions at 16 V_{pp} driving voltage amplitude. Vertical lines show peak values for the velocities from time-averaged LIF measurements.

Ion density measurements for the same driving amplitudes are presented in Fig. 6. Ion density oscillations become more coherent in time with the increase of the driving amplitude, but mean value of ion density does not change lot with amplitude. The deviation between the upper and the lower estimations of average density did not exceed 10%. This suggests that thrust, which is a function of density, does not change significantly during driving as well.

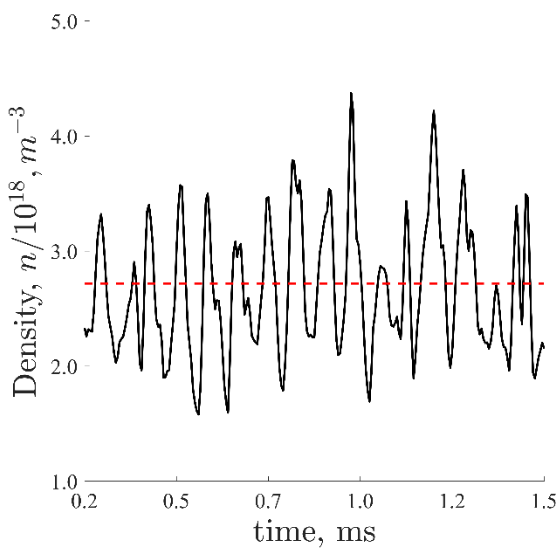

Figure 6. Ion density oscillations at 16V driving potential.

IV. 1D Hybrid-direct kinetic (DK) simulation

A one-dimensional (1D) hybrid-direct kinetic (DK) simulation is used to model the forced oscillation cases performed in experiments. The detail of the 1D hybrid-DK model is described in Ref. 8. The thruster assumed for the simulation is a SPT-100 type thruster, as the model is validated for these thrusters. Another important assumption is that the electron mobility model used in the model follows a “two-region” model [18] and non-magnetized electron transport near the anode [19]. A stable oscillation mode that gives a small-amplitude sinusoidal oscillation is found, and then an AC modulation is forced to the discharge voltage with a given amplitude and breathing mode oscillation observed in the DC discharge voltage case.

Figure 7 shows the thrust modulation as a function of the AC modulation amplitude of discharge voltage. Below 10% discharge voltage AC modulation, the discharge current and thrust oscillation show a “linear” mode [20, 21], i.e., relatively small amplitude oscillation. However, above 10%, the oscillation becomes nonlinear and tends to be in a pulse-type oscillation mode. It can also be seen that the thrust stays constant during the increase of AC amplitude modulation, but a slight increase of thrust is predicted in the linear mode. Once the nonlinear mode occurs, the time-averaged thrust slightly decreases, indicating that the efficiency decreases too.

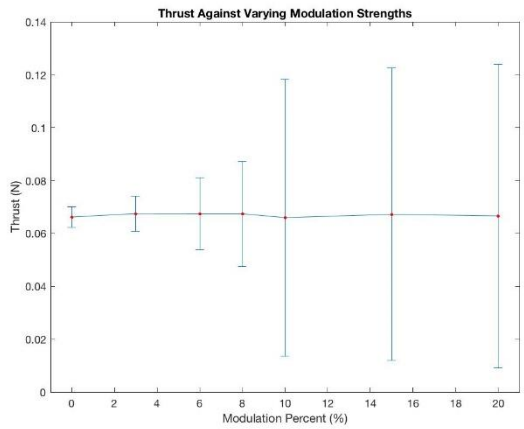

Figure 7. Thrust vs Modulation amplitude of the discharge voltage from simulation.

Figure 8 shows the temporal evolution of calculated thrust and imposed discharge voltage. The discharge current is a sinusoidal oscillation with frequency close to the breathing mode oscillation. The thrust shown here exhibits a coherent oscillation mode. The thrust (also discharge current) and discharge voltage are close to being in-phase.

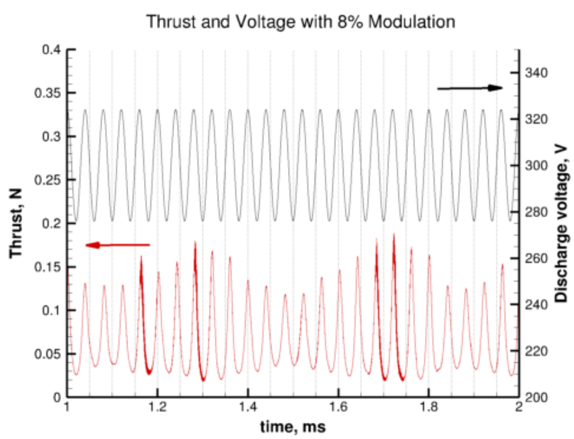

Figure 8. Temporal evolution of thrust and discharge voltage.

Figure 9 shows the total electron energy (sum of kinetic and thermal energies) as a function of space for different times during the oscillation. When the discharge voltage is maximum, there are higher power input to the system, so the electron energy increases particularly in the ionization region (i.e., x < 0.02 m, where 0.025 m is the channel exit). The electron energy becomes smaller when the discharge voltage is smaller. Therefore, it can be seen that the

AC discharge voltage modulation affects the electron dynamics and hence induces an ionization oscillation in the system.

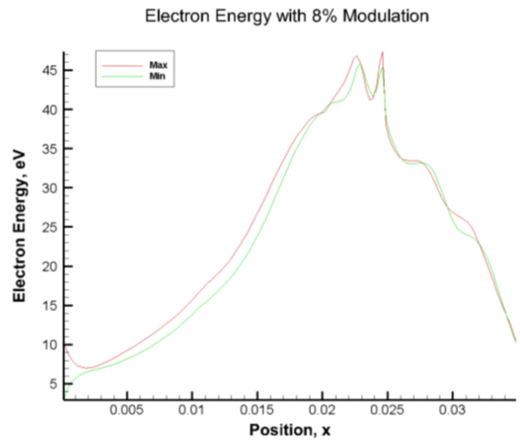

Figure 9. Spatial profile of electron total energy at the maximum and minimum of the discharge current oscillation.

The ion VDFs at downstream of the channel exit are shown in Fig. 10. There is a small density population at low velocity (~6,000 m/s) due to ionization taking place near the acceleration region. However, it is evident that the ion VDFs are correlated with the AC modulated discharge voltage. This qualitatively agrees with the experimental measurements shown in Figure 5, where the velocity at the peak of the IVDF moves accordingly with the discharge voltage. The ions are accelerated when the discharge voltage is large during the modulation.

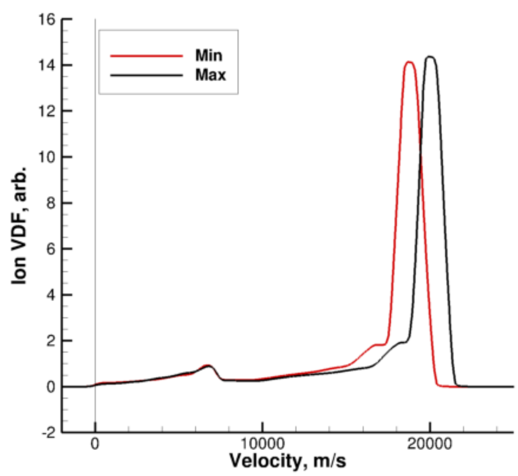

Figure 10. Normalized ion VDF at 5mm downstream of the channel exit.

V. Conclusion

In summary, the new time-resolver laser-induced fluorescence technique was developed and implemented for IVDF measurements on cylindrical Hall thruster during breathing oscillations. This approach allows to resolve low frequency oscillations in Hall plasma devices, such as breathing modes or spokes. Numerical simulations of a 1D Hall thruster discharge plasma are used to model the forced discharge voltage oscillation. In particular, the transition of IVDFs during the AC modulated discharge voltage shows good agreement. Numerical simulations of a cylindrical Hall thruster plasma are reserved for future work.

Next important step is to extend this approach from externally induced oscillations to naturally occurred quasi-coherent oscillations. Measurements of the discharge current and ion density show that with increase of the driving amplitude average values of these quantities remain approximately the same. Therefore, one can say that the driving of the anode potential with low amplitudes (less than 10% of total discharge voltage) can be used to actively control low frequency oscillations, without changes in average plasma behavior.

Acknowledgments

This work was partially supported by ASFOR and NSERC of Canada. We acknowledge Alex Merzhevskiy for his technical support. K.H. would like to acknowledge K. Ramadan for running and analyzing the simulations during the NSF Research Experiences for Undergraduate (REU) program at the Department of Aerospace Engineering at Texas A&M University. The simulations were run on the Texas A&M University supercomputing clusters.

References

[1] Martinez-Sanchez, M., and Pollard, J. E., "Spacecraft Electric Propulsion — An Overview," *Journal of Propulsion and Power*, Vol. 14, No. 5, pp. 688-699, 1998.

[2] Morozov, A. I., "The conceptual development of stationary plasma thrusters," *Plasma Phys. Rep.* Vol. 29, 2003, p.235.

[3] Goebel, D. M. and Katz, I., *Fundamentals of Electric Propulsion: Ion and Hall Thrusters*, Wiley, 2008.

[4] Choueiri, E. Y., "Plasma oscillations in hall thrusters," *Physics of Plasmas*, Vol. 8, No. 4, 2001, pp. 1411-1426.

[5] Zhurin, V., Kahn, J., Kaufman, H., Kozubsky, K., and Day, M., "Dynamic Characteristics of Closed Drift Thrusters," *IEPC-1993-095*, 1993

[6] Barral, S. and Ahedo, E., "On the Origin of Low Frequency Oscillations in Hall Thrusters," *AIP Conference Proceedings*, Vol. 993, 2008, pp. 439-442.

[7] Fife, J. M., *Hybrid-PIC Modeling and Electrostatic Probe Survey of Hall Thrusters*, Ph.D. thesis, MIT, 1998.

[8] Hara, K., Sekerak, M. J., Boyd, I. D., and Gallimore, A. D., "Mode transition of a Hall thruster discharge plasma," *Journal of Applied Physics*, Vol. 115, No. 20, 2014.

[9] Esipchuk, Yu. B., and Tilinin, G. N., "High-frequency plasma waves in a Hall accelerator with an extended acceleration zone," *Sov. Phys. Tech. Phys*., Vol. 22, 1977, pp. 974-978.

[10] Janes, G. S., Lowder, R. S., "Anomalous Electron Diffusion and Ion Acceleration in a Low-Density Plasma*," Physics of Fluids*, Vol. 9, No. 6, 1966, pp. 1115-1123.

[11] Boeuf, J. P., and Garrigues, L., "Low Frequency Oscillations in a Stationary Plasma Thruster," *Journal of Applied Physics*, Vol. 84, No. 7, 1998, pp. 3541-3554.

[12] Vaudolon, J., Balika, L., and Mazouffre. S., "Photon counting technique applied to time-resolved laser-induced fluorescence measurements on a stabilized discharge," *Review of Scientific Instruments*, Vol.84, No. 7, 2013, p. 073512.

[13] Durot, C. J., Gallimore, A. D., and Smith. T. B., "Development of a Novel Time-Resolved Laser-Induced Fluorescence Technique," *Review of Scientific Instruments*. Vol. 85, 2014, p. 013508.

[14] Diallo, A., Shi, Y., Keller, S., Raitses, Y., and Mazouffre, S., "Time-resolved ion velocity distribution in a cylindrical Hall thruster: Heterodyne-based experiment and modeling," *Review of Scientific Measurements*, Vol. 86, 2015, pp. 033506.

[15] Raitses Y., and Fisch. N. J., "Parametric investigations of a nonconventional hall thruster," *Physics of Plasmas*, Vol. 8, No. 5, 2001, pp. 2579-2586.

[16] Smirnov, A., Raitses, Y., and Fisch, N. J., "Parametric investigation of miniaturized cylindrical and annular hall thrusters," *Journal of Applied Physics*, Vol. 92, No. 10, 2002, pp. 5673-5679.

[17] Keller, S., Diallo, A., and Raitses, Y., "Laser-induced fluorescence measurements of driven breathing oscillations in a Hall thruster," New Orleans, LA, November 2014.

[18] Koo, J. W. and Boyd, I. D., "Modeling of anomalous electron mobility in Hall thrusters," Physics of Plasmas, Vol. 13, No. 3, 2006.

[19] Hara, K. and Boyd, I. D., "Low Frequency Oscillation Analysis of a Hall Thruster Using a One-Dimensional Hybrid-Direct Kinetic Simulation," 33rd International Electric Propulsion Conference, IEPC-2013-266, Washington D.C., October 2013.

[20] Barral, S. and Ahedo, E., "Low-frequency model of breathing oscillations in Hall discharges", Phys. Rev. E **79**, 046401, 2009.

[21] Hara, K., Keller, S., and Raitses, Y., "Measurements and theory of driven breathing oscillations in a Hall effect thruster," AIAA Propulsion and Energy Forum and Exposition, AIAA-2016-4532, Salt Lake City, UT, July 2016.